DONG THAP UNIVERSITY JOURNAL OF SCIENCE
Tạp chí Khoa học Đại học Đồng Tháp
Natural Sciences Issue
ISSN 0866-7675 | e-ISSN 2815-567X

DOI: https://doi.org/10.52714/dthu.ns.3182.1890

THE EFFECT OF TEMPERATURE ON THE STRUCTURE FORMATION OF $Ga_{0.2}N_{0.8}$ SEMICONDUCTOR MATERIAL USING MOLECULAR DYNAMICS SIMULATION.

Dung Nguyen Trong*, Hoang Thi Phuong, Ong Van Hoang, and Tran Thi Duyen

Faculty of Applied Science, University of Transport Technology
54 Trieu Khuc, Thanh Xuan, Hanoi, 100000, Vietnam
**Corresponding author, Email: dungnt78@utt.edu.vn*

Article history

Received: 23/02/2026; Received in revised form: 13/4/2026; Accepted: 15/4/2026

Abstract

This study investigates the effect of temperature on the structural evolution of $Ga_{0.2}N_{0.8}$ using large-scale molecular dynamics simulations involving 27436 atoms. The system was cooled from 300 K to 20 K at a rate of 4×10^{12} K/s using the MEAM interatomic potential. The results show that the system remains predominantly amorphous throughout the cooling process, with only minor fractions of HCP and BCC local structures. The total energy decreases from –287669 eV to –292264 eV, accompanied by a slight geometric shrinkage from 8.555 nm to 8.550 nm. The first peak of the radial distribution function remains at ~2.05 Å, indicating stable short-range bonding despite temperature variation. These findings demonstrate that the combination of non-stoichiometric composition and rapid cooling strongly suppresses crystallization and promotes structural "freezing" into an amorphous state. The study provides quantitative insight into the relationship between temperature, energy, and local structural ordering in Ga–N systems.

Keywords: *Ga–N semiconductor material, microstructure, molecular dynamics, temperature, total energy.*

Cite: Nguyen, T. D., Hoang, T. P., Ong, V. H., & Tran, T. D. (2026). The effect of temperature on the formation process structure of Ga0.2N0.8 semiconductor material using molecular dynamics simulation. *Dong Thap University Journal of Science*, *Online First*, 1-11. https://doi.org/10.52714/dthu.ns.3182.1890

NGHIÊN CỨU ẢNH HƯỞNG CỦA NHIỆT ĐỘ ĐẾN HÌNH THÀNH VI CẤU TRÚC CỦA VẬT LIỆU BÁN DẪN $Ga_{0.2}N_{0.8}$ BẰNG PHƯƠNG PHÁP MÔ PHỎNG ĐỘNG LỰC HỌC PHÂN TỬ

Nguyễn Trọng Dũng*, Hoàng Thị Phương[2], Ông Văn Hoàng[3] và Trần Thị Duyên[4]

Khoa Khoa học Ứng dụng, trường Đại học Công nghệ Giao thông Vận tải
54 Triều Khúc, Thanh Xuân, Hà Nội, 100000, Việt Nam.
**Tác giả liên hệ, Email: dungnt78@utt.edu.vn*

Lịch sử bài báo

Ngày nhận: 23/02/2026; Ngày nhận chỉnh sửa: 13/4/2026; Ngày duyệt đăng: 15/4/2026

Tóm tắt

Nghiên cứu này điều tra ảnh hưởng của nhiệt độ đến sự tiến hóa cấu trúc của $Ga_{0.2}N_{0.8}$ 27436 nguyên tử bằng cách sử dụng mô phỏng động lực học phân tử. Hệ thống được làm lạnh từ 300 K xuống 20 K với tốc độ 4×10^{12} K/s bằng cách sử dụng thế năng tương tác nguyên tử MEAM. Kết quả cho thấy hệ thống vẫn tồn tại chủ yếu ở trạng thái vô định hình trong suốt quá trình làm lạnh, chỉ có một phần nhỏ cấu trúc cục bộ HCP và BCC thay đổi. Tổng năng lượng giảm từ –287669 eV xuống –292264 eV, kèm theo sự co lại nhẹ về mặt hình học từ 8,555 nm xuống 8,550 nm. Đỉnh đầu tiên của hàm phân bố xuyên tâm vẫn ở mức ~2,05 Å, cho thấy liên kết tầm ngắn ổn định bất chấp sự thay đổi nhiệt độ. Những phát hiện này chứng minh rằng sự kết hợp giữa thành phần không cân bằng hóa học và quá trình làm lạnh nhanh sẽ ức chế mạnh mẽ quá trình kết tinh và thúc đẩy sự "đóng băng" cấu trúc thành trạng thái vô định hình. Nghiên cứu này cung cấp những hiểu biết định lượng về mối quan hệ giữa nhiệt độ, năng lượng và trật tự cấu trúc cục bộ trong hệ thống Ga–N.

Từ khóa: *động lực học phân tử, nhiệt độ, tổng năng lượng, vật liệu bán dẫn Ga–N, vi cấu trúc.*

1. Introduction

GaN is a semiconductor material with a large band gap of about 3.4 eV, widely used in optoelectronic devices, high-power transistors and light-emitting diodes (Wei et al., 2024). GaN is considered a potential candidate for applications at high frequencies and temperatures (Zhang et al., 2025). However, the structure of GaN is strongly influenced by many external factors such as temperature, doping composition and defect density, which strongly affect the physical properties and device performance (Yang et al., 2025). In particular, temperature has a great influence on the atomic structure of GaN. At high temperatures, anharmonic lattice vibrations reduce phonon lifetime and thermal conductivity through phonon-phonon scattering (Cuscó et al. 2015). The melting/decomposition process of GaN also depends greatly on temperature (Piechota et al., 2023). The mechanical properties of GaN, including plastic deformation and phase transition, are always greatly affected by temperature (Guo et al., 2020). Thus, temperature is not only a dependent factor but also a major factor controlling the stability and structural transformation of GaN. The formation of GaN structure in the solidification or amorphous state depends significantly on the cooling rate (Gao et al., 2018). Ishimaru et al., 1997 also successfully demonstrated that the cooling rate determines the formation of the crystal structure (Ishimaru et al., 1997). The relationship between order and disorder is a key factor governing the structural state of materials (Cai & Drabold 2011). Various methods have been developed to investigate material microstructure. Among them, X-ray diffraction is an experimental method that has successfully determined the Ga–N bond length to be 1.97–1.98 Å [10] . Molecular dynamics (MD) simulation shows that the size of the system (number of atoms) is a key factor determining the reliability of the results and the applicability of the material (Liang et al. 2015; Trong, Quoc, and Ţălu 2026). Besides the selection of research methods, the simulation method also depends heavily on the selection of appropriate atomic interaction potentials such as: Classical interaction potentials such as Tersoff (Moon & Hwang 2003), MEAM interaction potential (Zhou et al., 2017) or deep neural network-based potentials (Wu et al., 2024). Although numerous studies have investigated the structural evolution of GaN materials, limited attention has been given to non-stoichiometric systems with large simulation sizes and the combined effects of rapid cooling and composition on amorphous structure formation. Therefore, this study was conducted to systematically investigate the structural transformation of $Ga_{0.2}N_{0.8}$ under the influence of temperature. The results showing microstructural characteristics including material shape, structural shape, number of structural units and radial distribution function (RDF) will be analyzed to clarify. Compared to previous studies that primarily focused on near-stoichiometric GaN or systems with limited simulation sizes, this study focuses on $Ga_{0.2}N_{0.8}$ materials with large system sizes up to 27436 atoms, allowing for reliable description of short-range order. The novelty of this work lies in (i) revealing the dominant amorphous state in non-stoichiometric $Ga_{0.2}N_{0.8}$, (ii) identifying the structural "freezing" mechanism induced by rapid cooling, and (iii) establishing a quantitative correlation between total energy, geometric shrinkage, and RDF.

2. Research Methods

$Ga_{0.2}N_{0.8}$ semiconductor materials were studied by molecular dynamics (MD) simulation (Chen et al., 2018) on LAMMPS software (Karaaslan et al., 2020). The Ga–N interaction was described by MEAM potential according to Yanqiu and Shuyong (Do, Shin, & Lee 2009), ensuring the accuracy of binding energy, lattice constants, and elastic properties.

The validity of the MEAM potential is supported by the agreement between the simulated Ga–N bond length obtained from RDF (~2.05 Å) and experimental values (1.97–1.98 Å). Previous studies have also demonstrated that MEAM reliably reproduces structural stability and bonding characteristics in Ga–N systems, including non-stoichiometric compositions.

Three-dimensional periodic boundary conditions were applied to eliminate surface effects and analyze the structural order of the material (Chen et al., 2018) , according to equation (1).

$$E_{tot} = \frac{1}{2}\sum_{ij} V_{ij}\left(r_{ij}\right) + \sum_{i} F_i\left(\bar{\rho}_i\right),\ V\left(r_{ij}\right)=E_i\left(\frac{a}{r_{ij}}\right)^n,\ F_i\left(\rho\right) = A_i E_i^0 \rho \ln\rho ,$$
$$\rho_i^{\alpha(1)}\left(R\right) = e^{-b^*},\ b^* = \beta_i^{(l)}\left(\frac{R}{R_i^0 - 1}\right),\ \left(\bar{\rho}_i\right)^2 = \sum_{l=0}^{3} t_i^{(l)}\left(\rho_i^{(l)}\right)^2 \quad (1)$$

where r_{ij} is the distance between the i and j atoms, and the parameters and coefficients characterizing the material are summarized in Table 1.

Table 1. Parameters of $Ga_{0.2}N_{0.8}$ semiconductor materials.

Ga element							
Coefficient	$E_i^0(eV)$	R_i^0(Å)	α_i	A_i	$\beta_i^{(0)}$	$\beta_i^{(1)}$	a(Å)
	2.900	1.00	4.421	0.97	4.80	3.10	4.247
Coefficient	$\beta_i^{(2)}$	$\beta_i^{(3)}$	$t_i^{(0)}$	$t_i^{(1)}$	$t_i^{(2)}$	$t_i^{(3)}$	r_c
	6.00	0.50	1.00	2.72	2.06	-4.00	3.003
N element							
Coefficient	$E_i^0(eV)$	R_i^0(Å)	α_i	A_i	$\beta_i^{(0)}$	$\beta_i^{(1)}$	a(Å)
	4.88	2.700	3.719	1.80	2.20	1.70	1.100
Coefficient	$\beta_i^{(2)}$	$\beta_i^{(3)}$	$t_i^{(0)}$	$t_i^{(1)}$	$t_i^{(2)}$	$t_i^{(3)}$	r_c
	1.65	4.00	1.00	0.05	1.00	0.00	1.10

The $Ga_{0.2}N_{0.8}$ semiconductor material parameters were obtained from previously validated datasets (Do et al., 2009). The bulk material size (l) was calculated using Formula (2) (Trong & Long 2021):

$$l = \sqrt[3]{\frac{N}{\rho}} = \sqrt[3]{\frac{(m_{Ga}.n_{Ga} + m_N.n_N)}{\rho}} \quad (2)$$

where N is the total number of atoms, n is the number of Ga atoms; $m_{(Ga)}$ and $m_{(N)}$ are the atomic masses of Ga and N; ρ is fixed at 6.15 g/cm³ to ensure that the simulated cell density matches experimental GaN. Time integrals are performed using the velocity Verlet algorithm (Verlet, 1967). The structural phase is determined by common neighborhood analysis (CNA) (Qiu et al., 2017), while temperature and pressure are controlled by the Nosé–Hoover thermostat (Hoover 1985; Nosé 1984) in the NVT set.

The CNA method classifies atomic environments based on local bonding topology, allowing identification of FCC, HCP, BCC, and amorphous structures from atomic neighbor configurations.

The radial distribution function g(r) is calculated according to Equation (3) (Trong, Quoc, and Ţălu 2026).

$$g(r) = \frac{V}{N^2}\left\langle \frac{\sum_i n_i(r)}{4\pi r^2 \Delta r} \right\rangle \quad (3)$$

where g(r) is the radial distribution function (RDF), r is the distance between atoms, V is the system volume, $n_i(r)$ is the number of atoms at distance r; the sum is taken over all pairs of atoms.

In this study, the radial distribution function (RDF) is further used to analyze nearest-neighbor bond lengths, providing a quantitative measure of short-range order in the system. The simulation procedure consisted of three steps: (i) initialization of the cubic lattice cell $Ga_{0.2}N_{0.8}$ with random atomic velocities at 300 K; (ii) system equilibrium over 40,000 MD steps at 300 K to eliminate non-physical configurations; (iii) controlled cooling from 300 K to 20 K at a rate of 4×10^{12} K/s, time step of 1 fs, totaling 280000 MD steps, allowing for monitoring phase transitions and structural evolution during cooling. This methodological framework allows for the evaluation of the influence of doping concentration, system size, and temperature on the structural evolution, phase behavior, and energy of $Ga_{0.2}N_{0.8}$.

3. Results and discussion

3.1. Microstructure Characteristic Quantities

The microstructure characteristic quantities of the $Ga_{0.2}N_{0.8}$ semiconductor material with 27436 atoms, including 5487 Ga atoms (red) and 21949 N atoms (blue), are expressed through shape, structural shape, number of structural units, and radial distribution function. The following are the microstructure characteristic quantities of the $Ga_{0.2}N_{0.8}$ semiconductor material.

The results show that the $Ga_{0.2}N_{0.8}$ semiconductor material with 27436 atoms, including 5487 Ga atoms (red) and 21949 N atoms (blue), is placed in a cubic structure and is represented by its shape (Figure 1a). At 77 K, the system is analyzed under equilibrium conditions. The structure of the $Ga_{0.2}N_{0.8}$ system consists of four types of local configurations: FCC (red), HCP (blue), BCC (black), Amor (yellow) (Figure 1b), with the number of structural units being 0 FCC, 29 HCP, 29 BCC, and 27376 Amor (Figure 1c) and radial distribution function with the lengths of Ga-Ga, Ga-N, N-N bonds, with corresponding bond lengths of 2.65 Å, 2.05 Å, and 1.65 Å and corresponding radial

distribution function heights of 4.72, 7.36, 37.28. The Ga–N bond length results are in complete agreement with the experimental XRD values corresponding to 1.97 to 1.98 Å (Zhou, Jones, and Chu 2017). Figure 1 is further analyzed to clarify structural evolution; as MD results are deterministic, uncertainty is reflected through structural variation rather than statistical error bars.

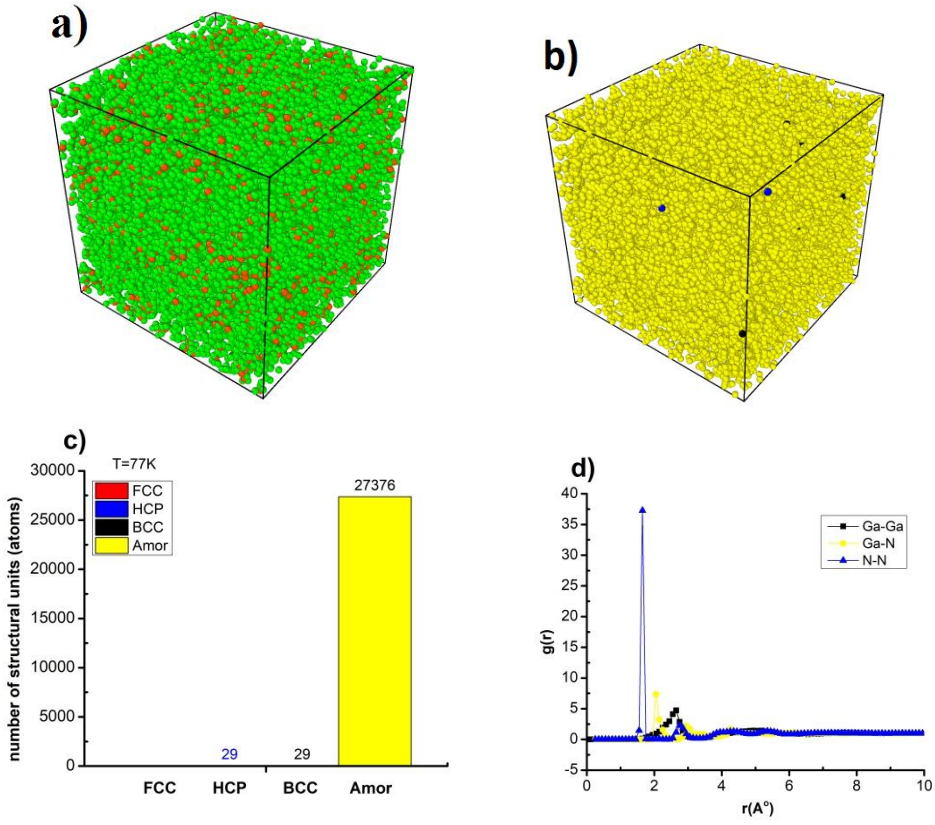

Figure 1 shows the microstructural characteristics of the $Ga_{0.2}N_{0.8}$ material with shape (a), structural shape (b), number of structural units (c), and radial distribution function (d) at 77 K.

3.2. Influence of Temperature

Based on the analysis of the microstructural characteristics of $Ga_{0.2}N_{0.8}$ material at 77 K, the following section focuses on clarifying the role of temperature influence on the structural evolution, total energy, and geometry of the system during cooling from 300 K to 20 K.

At 300 K, the $Ga_{0.2}N_{0.8}$ material has a structural shape (Figure 2a1) formed by four types of structures: FCC, HCP, BCC, Amor, with the corresponding number of structural units 1 FCC, 26 HCP, 32 BCC, 27376 Amor (Figure 2a2), and the corresponding Ga-N bond length $r_{Ga\text{-}N}$ = 2.05 Å (Figure 2a3). As the temperature decreases from 300 K to 20 K, a change in structural conformation occurs (Figure 2a1-2f1). This structural evolution leads to changes in the number of structural units (Figure 2a2-2f2), and the position of the first Ga–N RDF peak remains approximately constant at 2.05 Å, while the radial distribution function height increases from 7.66 to 10.28 (Figure 2a3-2f3).

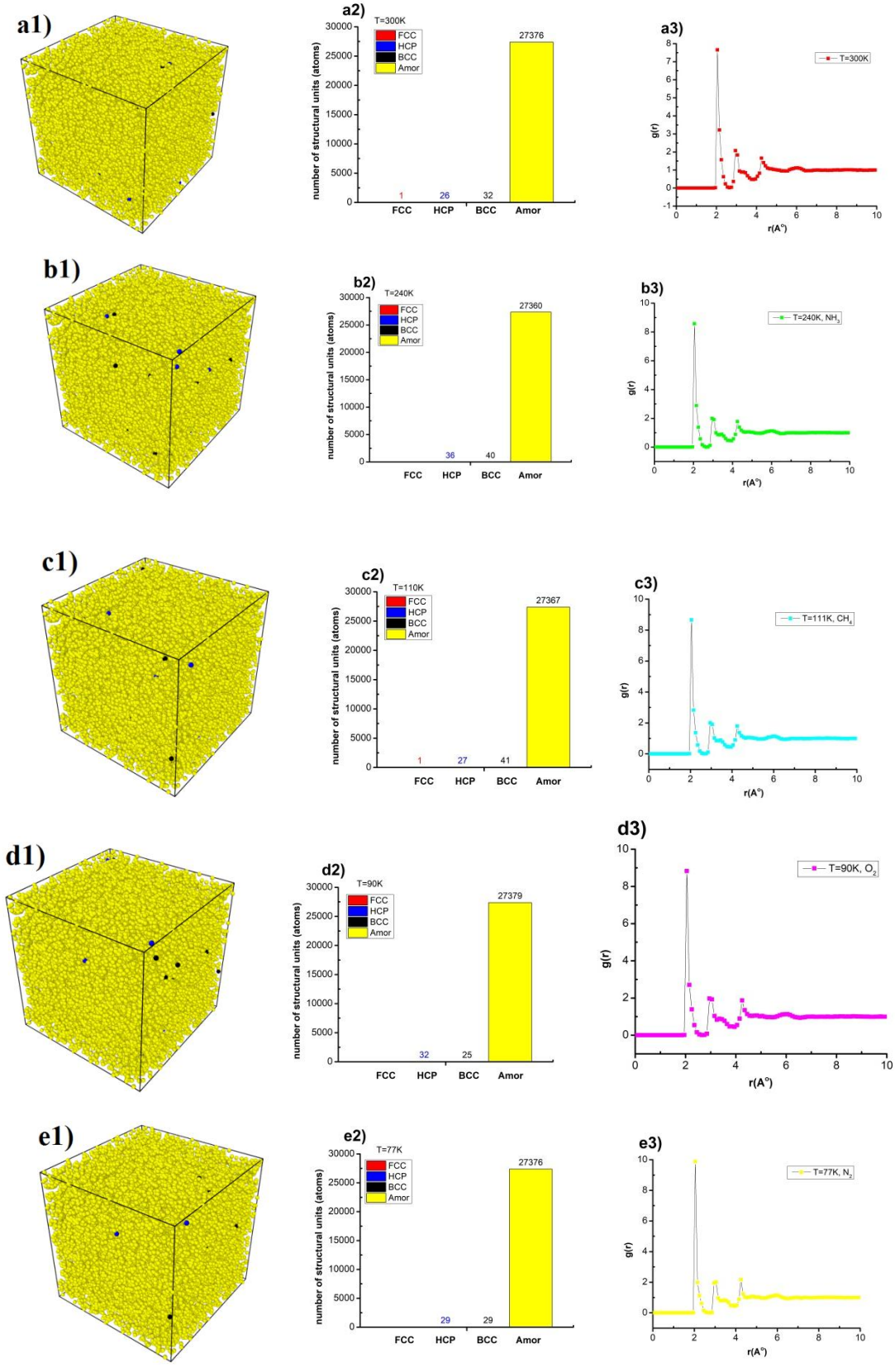
a1)
a2)
T=300K
FCC
HCP
BCC
Amor
number of structural units (atoms)
27376
1
26
32
FCC
HCP
BCC
Amor
a3)
T=300K
g(r)
r(A°)
b1)
b2)
T=240K
27360
36
40
b3)
T=240K, NH3
c1)
c2)
T=110K
27367
1
27
41
c3)
T=111K, CH4
d1)
d2)
T=90K
27379
32
25
d3)
T=90K, O2
e1)
e2)
T=77K
27376
29
29
e3)
T=77K, N2

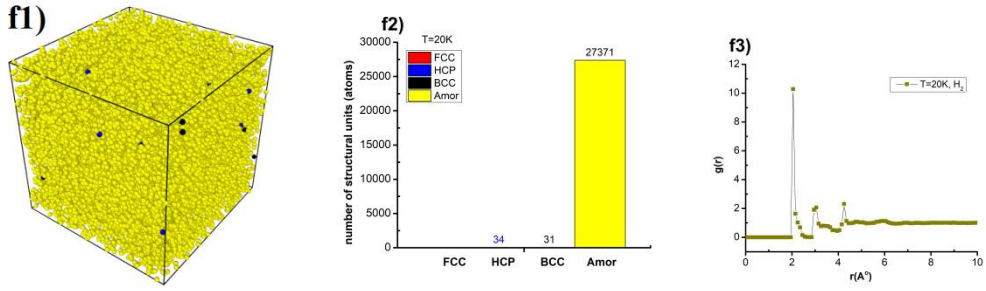

Figure 2 shows the microstructural characteristics of $Ga_{0.2}N_{0.8}$ material with shape (a1-f1), number of structural units (a2-f2), and bond length rGa-N (a3-f3) as the temperature decreases from 300 K to 20 K.

It should be clarified that the reported value of 2.05 Å corresponds to the position of the first RDF peak rather than a fixed bond length. Its weak temperature dependence arises from statistical averaging and the constraints of the interatomic potential, while thermal effects are reflected in peak broadening and intensity variation.

Mechanistically, the local increase in HCP and BCC structural units as the temperature decreases can be considered as intermediate structural states in the process of atomic rearrangement from the amorphous phase. FCC structural units appear at very low densities and rapidly disappear upon temperature reduction, indicating that this structure is not energetically stable in $Ga_{0.2}N_{0.8}$ semiconductors.

The cooling rate used in the simulation (4×10^{12} K/s) strongly restricts the diffusion of long-range atoms, preventing the system from achieving a crystalline equilibrium structure and instead "freezing" it in an amorphous state.

At lower cooling rates, increased atomic diffusion would likely promote crystallization and the development of long-range order, leading to different structural states.

This mechanism is consistent with previous conclusions about the dominant role of cooling rate in the formation of amorphous structures, and highlights the differences between $Ga_{0.2}N_{0.8}$ semiconductors and other GaN semiconductors. At 300 K, the system predominantly remains in an amorphous state with 27376 Amor units, while only a very small number of FCC, HCP, and BCC crystal structure units appear. The total energy at this temperature is –287669 eV, indicating that the system is still in a high-energy state due to strong thermal vibrations. The initial size of the material at 300 K is 8.555 nm, characteristic of the thermal expansion state of the atomic lattice. When the temperature decreases to 240 K and 111 K, the total energy decreases significantly to –289505 eV and –291501 eV, demonstrating that the system releases energy through atomic rearrangement. Simultaneously, the number of HCP and BCC structural units increased, while the number of FCC structural units almost disappeared, indicating the formation of short-range order, a characteristic sign of the pre-crystallization phase.

Here, short-range order is characterized by the first RDF peak corresponding to nearest-neighbor bond lengths, reflecting local structural stability during the cooling process.

According to the law of thermal shrinkage, as temperature decreases, the material size

decreases, leading to a reduction in size and an increase in atomic density. At lower temperatures (90 K, 77 K, and 20 K), the total energy continued to decrease to –291678 eV, –291783 eV, and –292264 eV, respectively, reaching a minimum value at 20 K, indicating that the atomic configuration approached its most stable state. Notably, the position of the Ga–N RDF first peak remained approximately constant at 2.05 Å throughout the entire temperature range studied, confirming that the structural changes mainly stemmed from geometric shrinkage of the material and spatial rearrangement of the structural units, rather than changes in the nature of the chemical bonds. At 77 K, the $Ga_{0.2}N_{0.8}$ system continued to exhibit thermal stability. The total energy of the material decreased to –291783 eV, lower than at higher temperatures, indicating that the atomic configuration was increasingly approaching the minimum energy state. The number of HCP and BCC structural units reached 29 HCP and 29 BCC, respectively, while the Amor phase remained absolutely dominant with 27376 Amor, confirming that the system had not undergone long-term crystallization but only formed local and intermediate order. Notably, the size of the $Ga_{0.2}N_{0.8}$ system at 77 K reached 8.555 nm, clearly reflecting the thermal shrinkage effect during cooling. This size reduction is consistent with the established simulation rule (for every 30 K decrease in temperature, the system size decreases by approximately 0.001 Å), increasing the atomic density and strengthening the Ga–N interaction. Compared with previous studies on GaN using MD simulations, the results at 77 K show some noteworthy differences. While many works report the formation of distinct crystal order during slow cooling, the $Ga_{0.2}N_{0.8}$ system in this study maintained a predominantly amorphous state, accompanied by limited appearance of HCP and BCC units. This suggests that the combined effect of non-stoichiometric chemical composition and high cooling rate inhibited long-term order development while promoting local and mid-range order formation. This result differs from pure GaN simulations, where crystalline structures generally predominate at the same temperature range. This indicates that the $Ga_{0.2}N_{0.8}$ system tends to be more strongly stable in the amorphous state, even at very low temperatures. This difference may stem from chemical imbalances and the uneven distribution of Ga and N atoms, increasing the degree of structural disorder and hindering long-term order formation. The obtained results add a new perspective on the role of composition and temperature in controlling the structural state of Ga–N materials.

4. Conclusion

In this study, the effect of temperature on microstructural formation and evolution of $Ga_{0.2}N_{0.8}$ semiconductor materials was systematically investigated using molecular dynamics simulation. The results demonstrate that as temperature decreases from 300 K to 20 K, the material system undergoes a significant thermodynamic stabilization process, evidenced by the continuous decrease in total energy and shrinkage of the system size. Specifically, the total energy decreases from –287669 eV to –292264 eV, while the material size decreases from 8.555 nm to 8.550 nm, reflecting the thermal shrinkage effect and the increase in atomic density. Structural analysis revealed that the amorphous phase predominated throughout the entire temperature range studied; however, the appearance and local increase of HCP and BCC structural units at low temperatures indicated the formation of short-range order. Notably, the position of the Ga–N RDF first peak remained approximately constant at 2.05 Å, which is in good agreement with experimental data, confirming that the structural changes mainly stemmed from geometric rearrangement and system shrinkage, rather than changes in the nature of the chemical bonds. This study quantitatively clarifies the relationship between temperature, total energy,

geometric shrinkage, and local order in large-scale $Ga_{0.2}N_{0.8}$ systems, providing an important theoretical basis for research and applications of Ga–N under low-temperature conditions.

Acknowledgements This research was funded by the University of Transport Technology (UTT), Viet Nam under grant number: ĐTTĐ2425-34.

Data Availability Statement: The data that support the findings of this study are available from the corresponding authors upon reasonable request.

Competing interests: The authors declare that they have no competing interests.

References

Ambacher, O. (1999). Properties of gallium nitride. INSPEC, London.

Cai, B., and Drabold, D.A. (2011). "Properties of Amorphous GaN from First-Principles Simulations." *Phys. Rev. B* 84(7): 075216.
https://doi.org/10.1103/PhysRevB.84.075216.

Chen, C., Haitao, L., Henggao, X., and Xianghe, P. (2018). "Molecular Dynamics Simulation on B3-GaN Thin Films under Nanoindentation." *Nanomaterials* 8(10): 856. https://doi.org/10.3390/nano8100856.

Cuscó, R,N., Domènech, A., Novikov, S., Foxon, C.T. and Artús, L. (2015). "Anharmonic Phonon Decay in Cubic GaN." *Phys. Rev. B* 92(7): 075206. https://doi.org/10.1103/PhysRevB.92.075206.

Do, E.C., Young, H.S., and Byeong, J.L. (2009). "Atomistic Modeling of III–V Nitrides: Modified Embedded-Atom Method Interatomic Potentials for GaN, InN and Ga1−xInxN." *Journal of Physics: Condensed Matter* 21(32): 325801. https://doi.org/10.1088/0953-8984/21/32/325801.

Gao, T., Kaiwen, L., Yidan, L., Xuechen, H., Lei, R., Xiangyang, L., and Quan, X. (2018). "Crystalline Structures and Defects in Liquid GaN during Rapid Cooling Processes." *Materials Science in Semiconductor Processing* 74: 46–50. https://doi.org/10.1016/j.mssp.2017.09.035.

Guo, J., Chen, J., and Wang, Y. (2020). "Temperature Effect on Mechanical Response of C-Plane Monocrystalline Gallium Nitride in Nanoindentation: A Molecular Dynamics Study." Ceram. Int. 46(8): 12686–12694. https://doi.org/10.1016/j.ceramint.2020.02.035.

Hoover, W.G. (1985). "Canonical Dynamics: Equilibrium Phase-Space Distributions." *Phys. Rev. A* 31(3): 1695–97. https://doi.org/10.1103/PhysRevA.31.1695.

Ishimaru, Manabu, Shinji Munetoh, and Teruaki Motooka. (1997). "Generation of Amorphous Silicon Structures by Rapid Quenching: A Molecular-Dynamics Study." *Phys. Rev. B* 56(23): 15133–38. https://doi.org/10.1103/PhysRevB.56.15133.

Karaaslan, Y., Haluk, Y., and Cem, S. (2020). "Assessment of Thermal Transport Properties of Group-III Nitrides: A Classical Molecular Dynamics Study with Transferable Tersoff-Type Interatomic Potentials." *Phys. Rev. Appl.* 13(3): 34027. https://doi.org/10.1103/PhysRevApplied.13.034027.

Liang, Z., Ankit, J., Alan, J.H.M., and Pawel, K. (2015). "Molecular Simulations and Lattice Dynamics Determination of Stillinger-Weber GaN Thermal Conductivity." *Journal of Applied Physics* 118(12): 125104. https://doi.org/10.1063/1.4931673.

Moon, W.H., and Ho, J.H. (2003). "Structural and Thermodynamic Properties of GaN: A Molecular Dynamics Simulation." *Physics Letters A* 315(3): 319–24. https://doi.org/10.1016/S0375-9601(03)01039-9.

Nosé, S. (1984). "A Unified Formulation of the Constant Temperature Molecular Dynamics Methods." *The Journal of Chemical Physics* 81(1): 511–19. https://doi.org/10.1063/1.447334.

Piechota, J., Stanisław, K., Bohdan, S., Petro, S., Sylwester, P., and Izabella, G. (2023). "Melting versus Decomposition of GaN: Ab Initio Molecular Dynamics Study and Comparison to Experimental Data." *Chemistry of Materials* 35(18): 7694–7707. https://doi.org/10.1021/acs.chemmater.3c01477.

Qiu, Y.Q., Wei, Y.C., Long, J.L, Jun, J.Y, Jie, W., and Qin, Z. (2017). "Structural, Electronic Properties with Different Terminations for Fluorapatite (001) Surface: A First-Principles Investigation." *Computational Materials Science* 126: 132–38. https://doi.org/10.1016/j.commatsci.2016.09.027.

Ştefan, Ţ., Trong, D.N., Lam, V.T. (2025). "The Power of Simulation: Exploring Binary Alloys for next-Generation Applications" *Journal of Nanomaterials and Applications (JNA)* 1(1): 1–16. https://doi.org/10.65273/hhit.jna.2025.1.1.1-16.

Trong, D.N., and Van, C.L. (2021). "Factors Affecting the Depth of the Earth's Surface on the Heterogeneous Dynamics of Cu_{1-x} Ni_x Alloy, x = 0.1, 0.3, 0.5, 0.7, 0.9 by Molecular Dynamics Simulation Method." *Materials Today Communications* 29: 102812. https://doi.org/10.1016/j.mtcomm.2021.102812.

Trong, D.N., Tuan, T.Q., and Ştefan, Ţ. (2026). "Simulation Study of Structural, Phase Transition, and Glass Transition Behavior in $Ga_{1-x}In_x$ Alloys (x = 0.2–0.8)." *Physica B: Condensed Matter* 727: 418271. https://doi.org/10.1016/j.physb.2026.418271.

Verlet, L. 1967. "Computer 'Experiments' on Classical Fluids. I. Thermodynamical Properties of Lennard-Jones Molecules." *Phys. Rev.* 159(1): 98–103. https://doi.org/10.1103/PhysRev.159.98.

Wei, B., Li, Y., Wang, L., Kai, W., Qiyang, S., Xiaolong, Y., Douglas, L.A., et al. (2024). "High-Order Phonon Anharmonicity and Thermal Conductivity in GaN." *Phys. Rev. B.* 109(15): 155204. https://doi.org/10.1103/PhysRevB.109.155204.

Wu, J., Zhou, E., An, H., Zhang, H., Ming, H., and Guangzhao, Q. (2024). "Deep-Potential Enabled Multiscale Simulation of Gallium Nitride Devices on Boron Arsenide Cooling Substrates." *Nature Communications* 15(1): 2540. https://doi.org/10.1038/s41467-024-46806-7.

Yang, J., Sun, Y., and Ben. X. (2025). "Impact of Point Defects on the Thermal Conductivity of GaN Studied Using Machine-Learned Potentials." *Phys. Rev. B* 111(10): 104112. https://doi.org/10.1103/PhysRevB.111.104112.

Zhang, Z., Zhenqiao, Z., Yingying, W., Zerui, Z., Zhonghan, Y., Wenjuan, X., Dan, Z., et al. (2025). "Effect of Temperature on the Nanoindentation Behavior of Single Crystal GaN by Molecular Dynamics Simulations." *Vacuum* 239: 114423. https://doi.org/10.1016/j.vacuum.2025.114423.

Zhou, X.W., Jones, R.E. and Chu, K. (2017). "Polymorphic Improvement of Stillinger-Weber Potential for InGaN." *Journal of Applied Physics* 122(23): 235703. https://doi.org/10.1063/1.5001339.